Systematic study of the spin stiffness dependence on Phosphorus alloying in (Ga,Mn)As ferromagnetic semiconductor

Sylvain Sylvain.Shihab@insp.Jussieu.Fr Shihab, Hassen Riahi, L. Thevenard, Hans Jürgen von Bardeleben, Aristide Lemaître, Catherine Gourdon

Systematic study of the spin stiffness dependence on Phosphorus alloying in (Ga,Mn)As ferromagnetic semiconductor

S. Shihab,[1,2] H. Riahi,[3] L. Thevenard,[1,2] H. J. von Bardeleben,[1,2] A. Lemaître,[4] and C. Gourdon[1,2]
[1)] *CNRS, UMR7588, Institut des Nanosciences de Paris, 4 place Jussieu, 75005 Paris, France*
[2)] *Sorbonne Universités, UPMC Université Paris 06, UMR7588, 4 place Jussieu, 75005 Paris, France*
[3)] *Laboratoire Matériaux Molécules et Applications, IPEST, Université de Carthage, La Marsa, Tunisie*
[4)] *Laboratoire de Photonique et Nanostructures, CNRS, UPR 20, Route de Nozay, 91460 Marcoussis, France*

(Dated: February 15, 2015)

We study the dependence of the spin stiffness constant on the phosphorus concentration in the ferromagnetic semiconductor (Ga,Mn)(As,P) with the aim of determining whether alloying with phosphorus is detrimental, neutral or advantageous to increase the spin stiffness. Time resolved magneto-optical experiments are carried out in thin epilayers. Laser pulses excite two perpendicular standing spin wave modes which are exchange related. We show that the first mode is spatially uniform across the layer corresponding to a $k \approx 0$ wavevector. From the two frequencies and k-vector spacings we obtain the spin stiffness constant for different phosphorus concentrations using weak surface pinning conditions. The mode assessment is checked by comparison with the spin stiffness obtained from domain pattern analysis for samples with out-of-plane magnetization and with ferromagnetic resonance experiments when more than one spin wave mode is observed. The spin stiffness is found to exhibit little variation with phosphorus concentration in contradiction with ab-initio predictions.

PACS numbers: 75.78.Jp,75.30.Ds,75.50.Pp

Building complex heterostructures, such as tunnel magnetic junctions, from the same host material is a challenge in order to reduce detrimental interface effects between different parts of a spintronic device. In this framework, diluted magnetic semiconductors (DMS) are a class of materials able to address this challenge[1]. More fundamentally, DMS and more specifically the III-V based (Ga,Mn)As have become in the past decade a benchmark material in order to achieve predictable tuning of magnetic properties. Levers such as the temperature[2], the carrier concentration[3,4] but also the strain applied on the magnetic layer[5,6] or alloying with phosphorus[7,8] have been used in order to change the micromagnetic properties, *e.g.* the Curie temperature T_C, the saturation magnetization M_s, and the magnetic easy axis.

Among these properties, the spin stiffness D is perhaps the most difficult to tune, despite theoretical guidelines[9]. An increase of the spin stiffness keeping constant magnitude of the magnetization M_s would mean larger exchange constant A ($A = DM_s/2$) and therefore larger domain wall width and domain wall velocity, this tunability remaining out of reach for metals. It is expected that alloying with phosphorus should increase the spin stiffness owing to an increase of Mn-hole exchange integral J_{pd}, the stronger hybridization of the p-d wave functions arising mainly from the smaller lattice constant of GaMnP[10]. The effect on T_C remains theoretically unclear. Whereas an overall increase is predicted from (Ga,Mn)As to (Ga,Mn)P[10,11], a decrease might occur for P concentration between zero and 25 %[11]. Furthermore it was shown experimentally, that (Ga,Mn)(As,P) suffers a metal-to-insulator transition with increasing Phosphorus concentration with a drop of its T_C[12,13]. A modest increase of D between $y = 0$ and $y > 6$ % can be inferred from results on the exchange constant A obtained for (Ga,Mn)(As,P) samples with out-of-plane easy axis using domain pattern analysis[14,15]. However recent results using an optical technique suggest a decrease of D with P alloying but with only one (Ga,Mn)(As,P) sample studied[16]. Unfortunately domain pattern analysis cannot be used to determine the spin stiffness for in-plane magnetized samples. To assess this value at low P concentration and in-plane easy axis, techniques based on excitation of exchange related perpendicular standing spin waves (PSSW) should instead be used. The spin stiffness constant can be extracted from the frequency spacing of excited modes. One technique is the standard ferromagnetic resonance (FMR)[4,17], another is the time-resolved magneto-optical Kerr effect experiment (TRMOKE)[6,16,18,19] recently pointed out as an optical analog of FMR for DMS[19]. However, the condition for PSSW detection is not the same for the two techniques. Some modes undetectable by FMR are observed by TRMOKE.

Here, we report on the determination of the spin stiffness constant by TRMOKE for samples with several P and Mn concentrations. In order to assess the mode k-vector we use the results previously obtained from domain pattern analysis for out-of-plane magnetized samples[15]. We obtain the variation of D with phosphorus concentration up to 9 %.

Samples used for this study are epilayers of

$(Ga_{1-x},Mn_x)(As_{1-y},P_y)$ grown on a (001) GaAs substrate and annealed 1 hour at 250°C. The thickness obtained from X-rays measurements is in the range 43-50nm. Samples from two sets with effective Mn concentration x_{eff} around 3.5 % and 5 % were studied. x_{eff} was determined from the saturation magnetization M_s measured by SQUID magnetometry. All samples were characterized beforehand by FMR[8]. Typical FMR spectra are displayed in the inset of Fig. 1, where only one PSSW mode is observed, as for most samples. This allows the determination of the magnetic anisotropy constants but precludes any estimation of the spin stiffness constant. TRMOKE experiments are carried out on in-plane magnetized samples with zero external magnetic field after a 60 mT initial preparation step. For out-of-plane samples an in-plane field is applied to pull the magnetization into the layer plane. The laser source is a Ti:Sa laser with pulse width ≈130 fs at wavelength λ=703 nm. The sample is glued on the cold finger of a liquid He flow cryostat. To limit thermal effects, experiments are performed at low pump and probe fluence (F_{pump}=1.1 μJ cm^{-2}, F_{probe} =0.4 μJ cm^{-2}), with a circularly or linearly pump beam, and a probe beam linearly polarized along the magnetization direction. At low temperature a pump induced stationary increase of temperature of 0.5 K is estimated. The magnetization dynamics is monitored through the Kerr rotation of the polarization detected by a balanced optical bridge.

A typical dynamical signal is shown in Fig. 1. After excitation by the pump beam at t=0, which generates a transient change of the anisotropy constants and therefore of the effective magnetic field, the magnetization is launched into precession and relaxes toward its equilibrium position in a few ns. The dynamical signal exhibits damped oscillations with two frequencies, representing optically generated spin wave modes (in some samples only one frequency is detected). For most of the samples, there is no difference between linearly and circularly polarized pump, except for two samples without P where the second spin-wave frequency was only observed in the helicity dependent signal. The TRMOKE signal is fitted by the relation:

$$S(t) = \sum_i A_i e^{\alpha_i 2\pi f_i t} \sin(2\pi f_i t + \phi_i)\,, \qquad (1)$$

where f_i is the frequency, ϕ_i the phase, A_i the amplitude and α_i the effective (inhomogeneous) damping of the i-th excited mode. The signal in Fig. 1 is obtained in a y=3.4 % sample at 12 K. Parameters from the fit are $f_1 = 1.11 \pm 0.02$ GHz, $f_2 = 4.03 \pm 0.05$ GHz , $\alpha_{1,2}$=0.08 and the amplitude ratio between the two modes is 0.3 .

To extract D from the observed frequencies, the magnetization dynamics is modeled in a standard way, starting from the Landau-Lifshitz-Gilbert equation with the exchange field and without damping[6,18]. For in-plane easy-axis, the equations for small precession angle of the

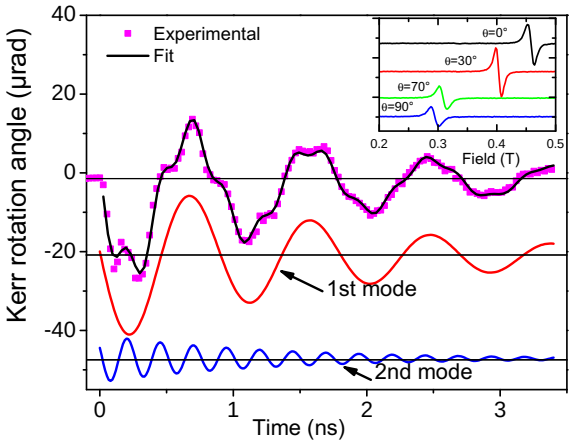

Figure 1. Typical dynamical signal obtained in TRMOKE experiments. The top curve displays the experimental signal (squares) and the associated fit (solid line) for (Ga,Mn)(As,P) with x_{eff} = 3.6% and y = 3.4% at T=12 K. The two curves below represent the oscillatory components of the experimental signal obtained from the fit of the signal, shifted for clarity. Inset: FMR spectra at T=4 K for different angles of an out-of-plane field (θ with respect to the [001] direction).

magnetization vector read:

$$\dot{\delta\theta} = \gamma\Big[-F_{\phi\phi}\delta\phi/M_s + D\frac{\partial^2\delta\phi}{\partial z^2}\Big]$$
$$\dot{\delta\phi} = \gamma\Big[F_{\theta\theta}\delta\theta/M_s - D\frac{\partial^2\delta\theta}{\partial z^2}\Big]\,, \qquad (2)$$

where the z-axis ($\parallel$ [001]) is perpendicular to the layer plane, and θ and ϕ are the polar and the azimuthal angles, respectively. $F_{ij} = \frac{\partial^2 F}{\partial i \partial j}|_{\phi=\phi_0}$ are the second derivatives of the magnetic energy with respect to the spherical coordinates using FMR convention[21] for the anisotropy constants K_i:

$$F_{\theta\theta} = -2K_{2\perp} + K_{4\parallel}\,(3+\cos 4\phi_0)\,/2 \qquad (3)$$
$$+2K_{2\parallel}\,(1-\sin 2\phi_0) + \mu_0 M_s^2$$
$$F_{\phi\phi} = 2\left(K_{4\parallel}\cos 4\phi_0 - K_{2\parallel}\cos 2\phi_0\right)\,, \qquad (4)$$

with ϕ_0 the equilibrium angle with respect to [100] given by $\sin 2\phi_0 = -K_{2\parallel}/K_{4\parallel}$ if $\left|K_{2\parallel}/K_{4\parallel}\right| < 1$ and $\phi_0 = \pi/4$ otherwise. For an out-of-plane easy axis and an in-plane applied magnetic field the above equations are modified to include the field. Calculations of the time dependent part gives the magnon dispersion relation:

$$f(k) = \frac{\gamma}{2\pi}\sqrt{F_{\theta\theta}F_{\phi\phi}/M_s^2 \pm (F_{\theta\theta}+F_{\phi\phi})Dk^2/M_s + D^2k^4}, \qquad (5)$$

where γ is the gyromagnetic ratio. The plus sign refers to a bulk mode ($\cos kz, \sin kz$) and the minus one to a surface mode ($\cosh kz, \sinh kz$). Note that by setting $D = 0$, one recovers the Smit-Beljers formula used for FMR[22]. The dispersion curve for a sample with y = 4.3% at T=12 K and H=0 is displayed in Fig. 2(a). The k = 0

frequency represents the spatially uniform mode and is related only to the anisotropy constants, while the curvature of the bulk mode dispersion curve depends on D.

The spatial dependence of $\delta\theta$ and $\delta\phi$ is calculated by finding the allowed confined surface-bulk hybridized spin wave wavevectors for a sample thickness L. Following Refs.[6,18], Rado-Weertman symmetric general boundary conditions for an in-plane magnetization are used[23]:

$$\frac{\partial\delta\phi}{\partial z}|_{\pm L/2} = 0 \quad \frac{\partial\delta\theta}{\partial z}|_{\pm L/2} = \mp\frac{2K_s}{DM_s}\delta\theta \quad , \qquad (6)$$

where $F_s = K_s \cos^2\theta$ is the surface anisotropy energy acting as a pinning term hindering the surface spin precession. The natural freedom condition ($K_s = 0$) gives a k-quantification in $n\pi/L$, where even (odd) n correspond to even (odd) spin wave modes. Given the experimental precession frequencies, the spin stiffness and the mode profiles are obtained through an iterative adjustment of D and K_s (Fig. 2(a)). D determines the frequency spacing between the two modes, while the pinning constant K_s shifts their frequencies.

In order to run this model, a preliminary step is to check the spatial profile of the lowest energy mode. To that end, a wet etching procedure was carried out on a $y = 4.3$ % sample in order to obtain a staircase pattern (Fig.2(c)). Successive oxidation and oxide removal sequences lead to a thickness difference of 5 nm between each step. The experimental results for this sample (Fig.2(c)) show that the first mode frequency does not change with decreasing thickness while the second one varies with the thickness as expected from Eqs. (5, 6). This shows firstly that the sample magnetic properties have a good in-depth and lateral uniformity and, secondly, that we are observing two exchange related PSSWs, where the first mode is a quasi-uniform mode as found from the mode profile calculation (Fig. 2(a) inset). Indeed we find a very small surface anisotropy constant $K_s = -1.3$ μJ m^{-2}, which divided by the layer thickness gives an equivalent bulk anisotropy constant 10 times smaller than the smallest bulk one (inset of Fig. 2(b)).

To compare FMR and optical experiments, we plot the frequencies obtained from TRMOKE and the $k = 0$ frequency calculated from the FMR anisotropy coefficients as a function of temperature. The result displayed in Fig.2(b) shows an excellent agreement between these two experiments for the first mode frequency. Such a comparison was shown for Nickel[20] and for (Ga,Mn)As at one temperature only[18] but, to our knowledge, it is the first time that such a good agreement on a large temperature range is demonstrated for DMS.

Because two PSSWs are generated, one can obtain D from the frequency spacing. However the correct value of D depends on the identification of the mode k-number (and thus symmetry) for the second excited spin wave. In a TRMOKE experiment, one is not able to discriminate between an odd or even mode. To determine the k-number, we compared the D value obtained from stripe domain analysis[15] for a $y = 8.8\%$ sample (perpendicular easy axis), $D = 11.8$ T nm^2, with the D values obtained from TRMOKE (under in-plane field) with the assumption of an even mode, $D = 5.4$ T nm^2, or an odd mode, $D = 21.6$ T nm^2. Results from these two experiments are in better agreement with the assumption of an even second mode. The larger D from domain pattern might arise from the assumption of Bloch domain walls whereas they are actually twisted Bloch-Néel walls[24]. Moreover,

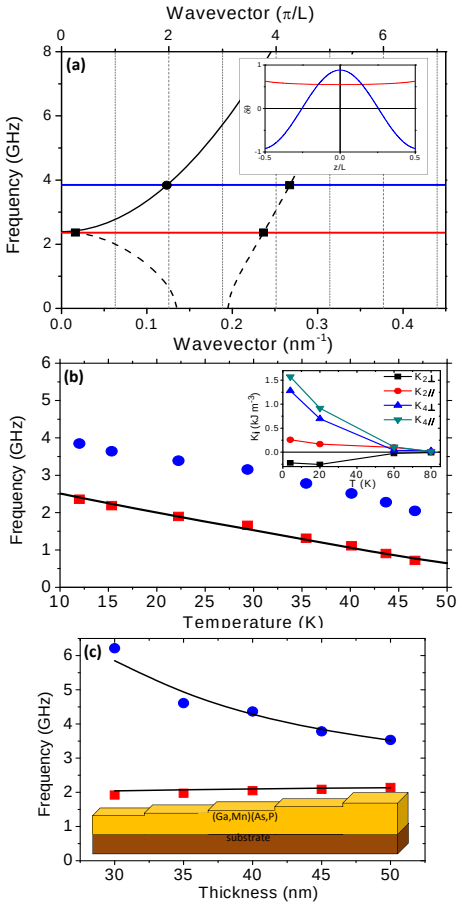

Figure 2. **(a)** Magnon dispersion relation showing the bulk modes (solid black line) and the surface modes (dashed black line) for a sample with $y = 4.3$ %, and L=50 nm. Horizontal lines represent the experimental frequencies (T=12 K). Squares (circles) represent the wavevectors of the bulk (surface) components of the spin waves found from the boundary conditions (Eq. 6). Inset: Mode profile (out-of-plane component $\delta\theta$) across the layer thickness for the first and second excited modes. **(b)** Frequencies of spin wave modes from TRMOKE (symbols) as a function of temperature, compared with the $k = 0$ frequency (solid line) calculated from FMR anisotropy constants (inset). **(c)** Layer thickness dependence of the frequencies of the two spin wave modes observed in TRMOKE experiments for a piece of the sample y=4.3 % (T=12 K). The solid lines are the frequencies calculated from Eq. (5, 6) using $D = 3.4$ T nm^2, and the anisotropy constants from FMR (inset of (b)). A sketch of the staircase-like sample after etching is shown below the curves.

assuming a second even mode, we find that the values obtained from TRMOKE and FMR are in good agreement for this sample, which shows two modes with both techniques (Fig. 3). This points to a good homogeneity of the sample since TRMOKE is a local probe (a few μm^2) whereas FMR probes the whole layer. Three GaMnAs samples (without phosphorus) have been studied. The D values obtained for two of them from TRMOKE (Fig. 3), and for the third one (on a GaInAs buffer, with perpendicular easy axis[14]) from domain pattern are all very close: 4.75, 4.8, and 5.1 T nm^2, respectively, which again is in favor of an even second PSSW mode in TRMOKE. Let us note that the spin stiffness values for GaMnAs reported in the literature are quite dispersed, some being comparable to ours[17,18], others, especially for thicker but likely inhomogeneous samples, being at least 3 times larger[4,18], or 4 times larger by TRMOKE but under the assumption of a second odd mode[16], which would give a value close to ours assuming an even second mode.

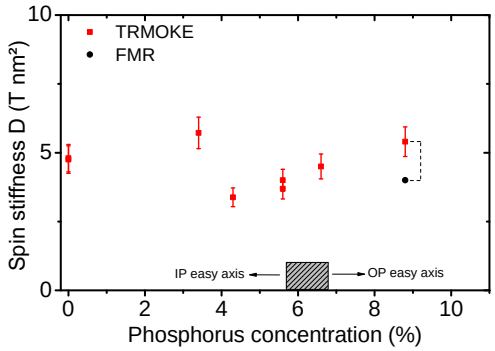

Figure 3. Dependence of the spin stiffness on the phosphorus concentration. Squares: from TRMOKE, circles: from FMR. The shaded zone indicates the frontier between samples with in-plane (IP) and out-of-plane (OP) easy magnetization axis. Data obtained from the same sample by different techniques are linked by a dashed line.

From TRMOKE results we obtain D for (Ga,Mn)(As,P) samples with y up to ≈9 % (Fig. 3). It is worth noticing that for two samples with the same phosphorus concentration (5.6 %) but different effective Mn concentrations (3.5 % and 5 %) we obtain the same spin stiffness. Indeed, by considering the spin stiffness $D = 2A/M_s$ and not only A one takes into account the effect of the effective Mn concentration, which ranges here from 3.5 % to 5.2 %. As can be seen in Fig. 3, D hardly varies with the Phosphorus concentration, *i.e.* with the lattice cell volume, which decreases with y. In simple models[1] D is expected to vary as $p^{1/3}J_{pd}^2$, where p is the carrier concentration. Our results can mean that J_{pd} does not increase with y. The increase of J_{pd} was predicted considering relaxed layers[10]. However, for pseudomorphic (Ga,Mn)(As,P) layers the lattice cell volume decrease is 40 % smaller, which may diminish the expected variation of J_{pd}. Alternatively a small increase of J_{pd} could be counterbalanced by a decrease of the carrier concentration as suggested in Ref. [13].

As a conclusion, we have carried out time-resolved magneto-optical experiment for (Ga,Mn)(As,P) samples. Together with previous results obtained for out-of-plane easy axis samples these results allow a determination of the spin stiffness constant for phosphorus concentration ranging continuously from zero up to 9 %. The spin stiffness is found to vary hardly with the phosphorus concentration. Incorporation of phosphorus is therefore neither detrimental nor advantageous to increase the spin stiffness.

We are grateful to H. Hurdequint from LPS-Orsay for fruitful discussions, to C. Testelin (INSP) for useful advices, and to M. Bernard and F. Breton (INSP) for technical assistance. This work has been supported by UPMC (Emergence 2012), by Region Ile-de-France (DIM Nano-K MURAS2012), by Agence Nationale de la Recherche (ANR 2010-BLANC-0424-02 and ANR13-JS04-0001-01), and by the French RENATECH network.

REFERENCES

[1] T. Dietl and H. Ohno, Rev. Mod. Phys. **86**, 187 (2014).
[2] M. Sawicki, F. Matsukura, A. Idziaszek, T. Dietl, G. Schott, C. Ruester, C. Gould, G. Karczewski, G. Schmidt, and L. Molenkamp, Phys. Rev. B **70**, 1 (2004).
[3] L. Thevenard, L. Largeau, O. Mauguin, and A. Lemaître, Phys. Rev. B **75**, 1 (2007).
[4] C. Bihler, W. Schoch, W. Limmer, S. T. B. Goennenwein, and M. S. Brandt, Phys. Rev. B **79**, 45205 (2009).
[5] A. W. Rushforth, E. De Ranieri, J. Zemen, J. Wunderlich, K. W. Edmonds, C. S. King, E. Ahmad, R. P. Campion, C. T. Foxon, B. L. Gallagher, K. Výborný, J. Kučera, and T. Jungwirth, Phys. Rev. B **78**, 085314 (2008).
[6] M. Bombeck, A. S. Salasyuk, B. A. Glavin, A. V. Scherbakov, C. Brüggemann, D. R. Yakovlev, V. F. Sapega, X. Liu, J. K. Furdyna, A. V. Akimov, and M. Bayer, Phys. Rev. B **85**, 195324 (2012).
[7] A. Lemaître, A. Miard, L. Travers, O. Mauguin, L. Largeau, C. Gourdon, V. Jeudy, M. Tran, and J.-M. George, Appl. Phys. Lett. 93, 021123 (2008).
[8] M. Cubukcu, H. J. von Bardeleben, K. Khazen, J. L. Cantin, O. Mauguin, L. Largeau, and A. Lemaître, Phys. Rev. B **81**, 041202 (2010).
[9] A. Werpachowska and T. Dietl, Phys. Rev. B **82**, 085204 (2010).
[10] J. Mašek, J. Kudrnovský, F. Máca, J. Sinova, A. MacDonald, R. Campion, B. Gallagher, and T. Jungwirth, Phys. Rev. B **75**, 045202 (2007).
[11] J. Xu and M. van Schilfgaarde, J. Mag. Magn. Mat. **305**, 63 (2006).
[12] P. R. Stone, K. Alberi, S. K. Z. Tardif, J.W. Beeman, K. M. Yu, W. Walukiewicz, and O. D. Dubon, Phys. Rev. Lett. 101, 087203 (2008).
[13] M. Cubukcu, H.J. von Bardeleben, J.L. Cantin, I. Vickridge, A. Lemaître, Thin Sol. Films 519, 8212, (2011)
[14] C. Gourdon, A. Dourlat, V. Jeudy, K. Khazen, H. von Bardeleben, L. Thevenard, and A. Lemaître, Phys. Rev. B **76**, 241301 (2007).
[15] S. Haghgoo, M. Cubukcu, H. J. von Bardeleben, L. Thevenard, A. Lemaître, and C. Gourdon, Phys. Rev. B **82**, 041301 (2010).
[16] N. Tesarova, D. Butkovicova, R. P. Campion, A. W. Rushforth, K. W. Edmonds, P. Wadley, B. L. Gallagher, E. Schmoranzerova, F. Trojanek, P. Maly, P. Motloch, V. Novak, T. Jungwirth, and P. Nemec, Phys. Rev. B **90**, 155203 (2014).

[17] X. Liu, Y. Zhou, and J. Furdyna, Phys. Rev. B **75**, 195220 (2007).
[18] D. Wang, Y. Ren, X. Liu, J. Furdyna, M. Grimsditch, and R. Merlin, Phys. Rev. B **75**, 233308 (2007).
[19] P. Němec, V. Novák, N. Tesařová, E. Rozkotová, H. Reichlová, D. Butkovičová, F. Trojánek, K. Olejník, P. Malý, R. P. Campion, B. L. Gallagher, J. Sinova, and T. Jungwirth, Nat. Com. **4**, 1422 (2013).
[20] M. van Kampen, C. Jozsa, J. Kohlhepp, P. LeClair, L. Lagae, W. de Jonge, and B. Koopmans, Phys. Rev. Lett. **88**, 227201 (2002).
[21] M. Farle, Rep. Prog. Phys. **61**, 755 (1998).
[22] J. Smith and H. G. Beljers, Phillips Res. Rep. 10, 113 (1955)
[23] G. T. Rado and J. R. Weertman, J. Phys. Chem. Sol. **11**, 315 (1959).
[24] L. Thevenard, C. Gourdon, S. Haghgoo, J-P. Adam, H. J. von Bardeleben, A. Lemaître, W. Schoch, and A. Thiaville, Phys. Rev. B **83**, 245211 (2011).